Postreplicative Joining of DNA Double-Strand Breaks Causes Genomic Instability in DNA-PKcs–Deficient Mouse Embryonic Fibroblasts

Marta Martín,[1] Anna Genescà,[1] Laura Latre,[1] Isabel Jaco,[2] Guillermo E. Taccioli,[3] Josep Egozcue,[1] María A. Blasco,[2] George Iliakis,[4] and Laura Tusell[1]

[1]Department of Cell Biology, Physiology, and Immunology, Institute of Biotechnology and Biomedicine, Universitat Autònoma de Barcelona, Bellaterra, Spain; [2]Molecular Oncology Program, Spanish National Cancer Centre, Madrid, Spain; [3]Department of Microbiology, Boston University School of Medicine, Boston, Massachussetts; and [4]Institute of Medical Radiation Biology, University Duisburg-Essen Medical School, Essen, Germany

Abstract

Combined cytogenetic and biochemical approaches were used to investigate the contributions of the catalytic subunit of DNA-dependent protein kinase (DNA-PKcs) in the maintenance of genomic stability in nonirradiated and irradiated primary mouse embryo fibroblasts (MEF). We show that telomere dysfunction contributes only marginally to genomic instability associated with DNA-PKcs deficiency in the absence of radiation. Following exposure to ionizing radiation, DNA-PKcs$^{-/-}$ MEFs are radiosensitized mainly as a result of the associated DNA double-strand break (DSB) repair defect. This defect manifests as an increase in the fraction of DSB rejoining with slow kinetics although nearly complete rejoining is achieved within 48 hours. Fifty-four hours after ionizing radiation, DNA-PKcs$^{-/-}$ cells present with a high number of simple and complex chromosome rearrangements as well as with unrepaired chromosome breaks. Overall, induction of chromosome aberrations is 6-fold higher in DNA-PKcs$^{-/-}$ MEFs than in their wild-type counterparts. Spectral karyotyping-fluorescence *in situ* hybridization technology distinguishes between rearrangements formed by prereplicative and postreplicative DSB rejoining and identifies sister chromatid fusion as a significant source of genomic instability and radiation sensitivity in DNA-PKcs$^{-/-}$ MEFs. Because DNA-PKcs$^{-/-}$ MEFs show a strong G_1 checkpoint response after ionizing radiation, we propose that the delayed rejoining of DNA DSBs in DNA-PKcs$^{-/-}$ MEFs prolongs the mean life of broken chromosome ends and increases the probability of incorrect joining. The preponderance of sister chromatid fusion as a product of incorrect joining points to a possible defect in S-phase arrest and emphasizes proximity in these misrepair events. (Cancer Res 2005; 65(22): 10223-32)

Introduction

The vast majority of human cancers are genetically unstable. This genomic instability can take two different forms (1). Most cancer cells are unable to maintain chromosomal integrity and display gross abnormalities in their karyotype (2–4). In a few cases, the instability is observed at the nucleotide level and is the result of faulty DNA repair (nucleotide-excision repair and mismatch repair), giving rise to base substitutions or deletions or insertions of a few nucleotides (5–9). The term genomic instability includes both forms of instability and can be defined as the continuous formation of new chromosome aberrations and mutations. This article focuses on the first form of instability, which results from the illegitimate rejoining of DNA double-strand breaks (DSB), generating, among other chromosome abnormalities, dicentric chromosomes and rings. These unstable chromosome forms can break during anaphase if they are pulled to opposite poles, generating the potential for new chromosome rearrangements in proliferating cells.

To maintain the integrity and stability of the genome, eukaryotic cells have developed at least two efficient pathways of DSB repair: nonhomologous end joining and homologous recombination (10–12). The main mechanism of DSB repair in mammalian cells is nonhomologous end joining. Six of the gene products required for nonhomologous end joining have been identified: Ku70 and Ku80, which form the Ku heterodimer that binds to DNA ends; the catalytic subunit of DNA-dependent protein kinase (DNA-PKcs), which is recruited by the Ku heterodimer to DNA ends and which brings the ends together in a synaptic complex; XRCC4 and DNA ligase IV, which form a heterodimer with DNA ligase activity; and Artemis, which is thought to be involved in the processing of DNA ends (10). As expected, inactivation of the genes involved in nonhomologous end joining impairs DSB rejoining, causes radiosensitivity to killing, and predisposes to cancer. Loss of DNA-PKcs or Ku70 has been associated with increased rates of lymphomas in mice (13). This phenotype is exacerbated when nonhomologous end joining–deficient mice also lack p53 (14, 15). Humans are likely to be no exception and defects in nonhomologous end joining leading to genomic instability may result in cancer predisposition and, importantly, may also increase the sensitivity of patients to therapies utilizing agents inducing DSBs. Indeed, a leukemia patient with a *DNA ligase IV* mutation who died from radiation sensitivity was reported by Riballo et al. (16). Recently, two new genomic instability disorders directly related to nonhomologous end joining defects have been reported (17), extending thus the importance of nonhomologous end joining repair pathways to human health. The first disorder included several groups of patients with severe combined immunodeficiency resulting from defects in Artemis (18, 19). These patients show predisposition to B-cell lymphomas (20). The second disorder included five patients with hypomorphic mutations in *DNA ligase IV* (21), one of whom developed leukemia (16).

Equally important as the efficient and correct repair of DSBs is the presence of functional telomeres, the nucleoprotein structures located at the ends of the chromosomes that prevent their fusion (joining) with other chromosome ends. Telomere

Requests for reprints: Anna Genescà, Cell Biology Unit, Ed CS, Universitat Autònoma de Barcelona, Bellaterra, Spain. Phone: 34-93-581-1498; Fax: 34-93-581-2295; E-mail: anna.genesca@uab.es.

doi:10.1158/0008-5472.CAN-05-0932

dysfunction, either by excessive replication-dependent erosion of telomeric DNA or by loss of proteins in the telomeric loop structure, leads to chromosome end-to-end fusions which, on entering into fusion-bridge-breakage cycles, generate genomic instability that may contribute to carcinogenesis (22–24). Several nonhomologous end joining components such as Ku and DNA-PKcs contribute to the formation of functional telomeres. Telomeric dysfunction, due either to the loss of proteins involved in the telomeric protective loop structure or to telomeric DNA erosion, is sensed as a DSB by DNA damage response proteins (25, 26). In addition, unprotected telomeres act as DSBs not only by joining to other uncapped telomeres forming telomere-telomere fusions (24, 27, 28) but also by joining to radiation-induced DSBs, thus forming telomere-DSB fusions (29, 30). Both kinds of fusions can generate genomic instability and are therefore potentially tumorigenic.

To evaluate the contribution of the two distinct functions (i.e., DSB repair versus telomere protection) of DNA-PKcs in genomic stability, we used spectral karyotyping-fluorescence *in situ* hybridization (SKY-FISH) technology to analyze metaphase chromosomes of primary mouse embryo fibroblasts (MEF) obtained from mice in which the *DNA-PKcs* gene was ablated by homologous recombination (31). The results suggest that DNA-PKcs–mediated telomere dysfunction contributes only marginally to radiation sensitivity and genomic instability in primary MEFs. Most importantly, we identify postreplicative joining of broken sister chromatids as an important source of genomic instability and radiation sensitivity in DNA-PKcs–deficient MEFs.

Materials and Methods

Radiation exposure and cell culture. DNA-PKcs null mice (DNA-PKcs$^{-/-}$) and wild-type animals (DNA-PKcs$^{+/+}$) were used. For genetic studies, pregnant DNA-PKcs$^{-/-}$ and DNA-PKcs$^{+/+}$ females were irradiated on days 12 to 14 of gestation with a 2-Gy dose under a ^{60}Co source. Six hours after ionizing radiation, females were sacrificed and a cell suspension was obtained from each littermate embryo, which was incubated in DMEM (Synovis Life Technologies, St. Paul, MN). After 24 hours, cell cultures were washed with PBS to isolate the MEFs and were further incubated at 37°C in a 10% CO_2 atmosphere. For biochemical studies, irradiation was done *in vitro* to better control time for kinetic studies of DBS rejoining.

Spectral karyotyping. Colcemid (KaryoMAX, Life Technologies, Inc.; final concentration, 0.14 μg/mL) was added to irradiated DNA-PKcs$^{-/-}$ and DNA-PKcs$^{+/+}$ MEF cultures at 48 hours postirradiation and allowed to act for 4 to 6 hours. Metaphase chromosome suspensions were then obtained after hypotonic shock and methanol-acetic acid fixation. These were kept at −20°C until slide dropping. The SKY-FISH technique allows the simultaneous and differential painting of all mouse (20 pairs) chromosomes. SKY was applied on metaphase chromosome spreads following the instructions of the manufacturer. Images were captured with a Nikon ECLIPSE E800 microscope equipped with a Cohu camera and the SkyView 2.1 (Applied Spectral Imaging, Inc., Migdad Ha'Emek, Israel) software. The coordinates of each metaphase analyzed in this way were noted for later relocation.

Telomere labeling. After SKY analysis, labeling of telomeric sequences onto the same slides was applied as described by Martin et al. (32). FISH was done using a Cy3-labeled $(CCCTAA)_3$ peptide nucleic acid probe (Perseptive Biosystems, Framingham, MA). Metaphases were relocalized and recaptured using an Olympus BX 60 microscope equipped with a Cohu camera and Smart Capture (Vysis, Inc., Downers Grove, IL) software.

Scoring of aberrations. *Telomere-telomere fusions* were scored using stringent criteria. We scored only those events in which the telomeres of adjoining chromosomes had fused into a single signal or in which no telomere signals at the joining point could be observed. In the first case, telomere-telomere fusions containing TTAGGG repeats at the fusion point would indicate dysfunctional telomeres that have fused due to the loss of the telomeric capping structure. In the second case, fusion of whole chromosomes without TTAGGG repeats at the fusion point provides evidence of a telomere-shortening phenomenon. In this latter case, special care was taken to ensure that the chromosomes involved in this type of fusion were not broken or rearranged. *Telomere-DSB fusions* are rearrangements resulting from a dysfunctional telomere joined to a broken end. These rearrangements will be identified by the joining point: in a telomere-DSB fusion, a broken chromosome end is joined to a dysfunctional telomere of another chromosome. *Break-produced aberrations* include all conventional exchange type aberrations such as translocations, dicentric chromosomes, interstitial deletions, etc., as well as nonexchange type aberrations such as chromosome and chromatid breaks. In the case of translocations, each translocated chromosome and its reciprocal translocation, or the unrejoined centric and acentric fragment, were considered as a single aberration. Similarly, each dicentric chromosome and the accompanying compound acentric fragment, or the two unrejoined acentric fragments, were also considered as a single aberration. We considered as interstitial deletions chromosomes with visibly deleted interstitial segments showing a complete set of telomeres and accompanied or not by an acentric fragment from the same chromosome with no telomeres. Isodicentric chromosomes and isoacentric fragments were painted in a single color after SKY-FISH and the reverse 4′,6-diamidino-2-phenylindole (DAPI) image, also provided by SKY-FISH, revealed a horizontal mirror image banding pattern.

Follow-up of the number of cell divisions after ionizing radiation. For SKY-FISH cytogenetic studies, MEFs were grown *in vitro* for 48 hours after female sacrifice. This time period favors the obtention of first and second mitosis after ionizing radiation. For sister chromatid fusion analysis, care was given in analyzing mainly first mitosis after irradiation. With this aim, MEFs were cultured in the presence of BrdUrd and metaphases were obtained at different time points after irradiation. After metaphase obtention, the BrdUrd + Hoechst 33258 protocol was applied as described by Martin et al. (32) and the slides with a frequency of first metaphases after irradiation higher than 75% were selected.

Sister chromatid fusion analysis. To analyze sister chromatid fusion on the previous selected slides, two consecutive stainings were applied. First, slides were solid stained with Leishman, which highly preserves the original chromosome morphology, thus providing a tool to observe the fusion of chromatids with detail. Centric and acentric fragments—presumably forming sister chromatid fusion—were identified during solid-staining analysis by the characteristic rounded aspect of one of their ends. Metaphase spreads were captured and their coordinates noted for later relocation. Subsequently, slides were processed for telomere labeling with peptide nucleic acid-FISH probes. Centric and acentric fragments with presumably fused chromatids in the solid-staining analysis were relocated and sister chromatid fusion was then confirmed with telomeric FISH analysis by the absence of telomere signals at fusion point.

Nucleoplasmic bridge analysis. Binucleated MEFs for nucleoplasmic bridge analysis were obtained by addition of cytochalasin B (Sigma) to irradiated DNA-PKcs$^{-/-}$ and DNA-PKcs$^{+/+}$ MEF cultures at 40 hours postirradiation to a final concentration of 6 μg/mL to block cytokinesis. Cells were trypsinized at 71 hours postirradiation, centrifuged, resuspended in cold hypotonic solution, and gently fixed in methanol-acetic acid. Binucleated MEF suspension was kept at −20°C until slide dropping. For binucleated MEF analysis, slides from irradiated DNA-PKcs$^{-/-}$ and DNA-PKcs$^{+/+}$ cells were Leishman solid-stained, which provides a well-defined shape for the nuclei and an unambiguous identification of the nucleoplasmic bridges. Binucleated MEFs presenting nucleoplasmic bridges were captured and coordinates were noted for relocalization after telomeric FISH labeling. After solid-staining analysis, slides were washed in PBS, treated with pepsin, and fixed with 4% formaldehyde. Telomere labeling was applied as described before (32). Telomere-labeled binucleated MEFs were recaptured and analyzed.

Asymmetrical field inversion gel electrophoresis. For the evaluation of DSB repair kinetics, DNA-PKcs$^{-/-}$ and DNA-PKcs$^{+/+}$ MEFs were cultured *in vitro* until confluence. Cells were cooled to 4°C before irradiation and were irradiated on ice using a Pantak X-ray machine MXR-321, operated at 320 kV and 10 mA with a 1.65-mm aluminum filter. After irradiation, cells were returned to the incubator at 37°C to allow for repair. After each repair time interval, cells were trypsinized, centrifuged, washed with PBS, centrifuged again, and resuspended at a final concentration of 2×10^6 cells/mL. This cell suspension was mixed with an equal volume of 1% low melting point agarose (Bio-Rad Laboratories, Hercules, CA) previously diluted in the cell culture medium and supplemented with 20 mmol/L HEPES and 5 mmol/L $NaHCO_3$. The mixed suspension was then pipetted into 3-mm-diameter glass tubes and placed on ice to allow solidification. The solidified cell-agarose suspension was extruded from the glass tubes and cut into 3×0.5 mm cylindrical blocks. Blocks were placed in lysis buffer containing 10 mmol/L Tris-HCl, 100 mmol/L EDTA, 50 mmol/L NaCl (pH 7.6), 2% *N*-lauryl-sarcosyl, 0.2 mg/mL protease (Sigma), and incubated at 50°C for 20 hours. After lysis, agarose blocks were washed for 1 hour at 37°C in a buffer containing 10 mmol/L Tris-HCl, 100 mmol/L EDTA, and 50 mmol/L NaCl (pH 7.6) and were then treated in the same buffer with 0.1 mg/mL RNase A.

Asymmetrical field inversion gel electrophoresis (FIGE) was carried out in 0.5% pure-grade agarose (Bio-Rad) gels, which were cast in the presence of 0.3 μg/mL ethidium bromide in 0.5 × Tris-borate EDTA at 8°C for 40 hours. During this time, cycles of 1.25 V/cm for 900 seconds in the direction of DNA migration alternated with cycles of 5.0 V/cm for 75 seconds in the reverse direction. The agarose gels were scanned immediately after running and were quantified to estimate DNA damage using ImageQuant 5.2 (Amersham Biosciences Corp., Piscataway, NJ) software.

DNA DSBs were quantified by calculating the fraction of activity released from the well into the lane (FAR) in irradiated and nonirradiated samples. The FAR measured in nonirradiated cells (background) was subtracted from the results shown with irradiated cells.

Cell cycle analysis. For cell cycle analysis, asynchronous exponentially growing DNA-PKcs$^{-/-}$ and DNA-PKcs$^{+/+}$ MEFs (passage 2-4) at 50% to 60% confluence were irradiated with 7 Gy of γ-rays and collected at different times after irradiation. Cells were trypsinized, centrifuged, washed in PBS, and fixed in 70% ethanol. After fixation, cells were stained with propidium iodide to perform analysis by flow cytometry. Activation of the G_1 checkpoint was evaluated by the decrease in the proportion of S-phase cells and by the increase in G_1/S ratio as a function of time after irradiation. The ratio G_1/S was used to indicate the concomitant modification in cell fraction in both phases of the cell cycle, which are expected to be modified in response to the activation of the G_1 checkpoint.

Results

Impaired DNA double-strand break repair contributes predominantly—and telomere dysfunction contributes marginally—both to spontaneous and radiation-induced chromosomal aberrations in DNA-PKcs–deficient primary mouse embryo fibroblasts. Most mammalian cells and mice deficient in any of the components of the nonhomologous end joining, such as DNA-PKcs, Ku, and Ligase IV, are hypersensitive to ionizing radiation. To investigate the contribution of telomeric versus repair functions of DNA-PKcs to the radiosensitivity of DNA-PKcs–deficient mice, we generated MEFs from pregnant females immediately after ionizing radiation at days 12 to 14 of gestation. Table 1 and Fig. 1*A* show the results of the cytogenetic analysis. The rate of spontaneous chromosome aberrations was higher in DNA-PKcs$^{-/-}$ than in wild-type MEFs. After ionizing radiation, this frequency was 6-fold higher in DNA-PKcs$^{-/-}$ MEFs than in their wild-type counterparts. Among the aberrations observed in DNA-PKcs$^{-/-}$ MEFs, those derived from chromosome breakage were more frequent than telomere-telomere fusions, which are indicative of telomere dysfunction. In the irradiated DNA-PKcs–deficient MEFs, we scored 1.41 break-produced aberrations per cell (Fig. 1*B*) but <1 telomere-telomere fusion per 20 cells, which translates to 0.04 per cell (Fig. 1*C*). Telomere-telomere fusions were only observed in DNA-PKcs$^{-/-}$ MEFs, indicating that our scoring criteria are stringent enough to avoid false positives. The frequency of telomere-telomere fusions observed in this study was low compared with other studies using primary or immortalized DNA-PKcs–deficient MEFs irradiated *in vitro* (24, 27). Thirteen of the fourteen observed telomere-telomere fusions contained TTAGGG repeats at the point of fusion (Fig. 1*C*), indicating that they were due to a loss of the telomeric capping structure rather than to telomeric shortening. Only one cell contained a chromosome aberration resulting from a dysfunctional telomere joined to a broken chromosome end (Fig. 1*D*). On the other hand, chromosome aberrations deriving exclusively from DNA breakage represented 77.3% of total spontaneous aberrations in nonirradiated DNA-PKcs$^{-/-}$ MEFs and 96.3% of the total aberrations in the irradiated knockouts (Table 1; Fig. 1*A*). Because the nonhomologous end joining defect is obvious in DNA-PKcs$^{-/-}$ MEFs, we analyzed exchange and nonexchange type chromosome aberrations in the two genetic backgrounds (Table 1). Spontaneous aberrations in the nonirradiated DNA-PKcs$^{-/-}$ MEFs were mainly of the nonexchange type (unrejoined breaks and fragments). Similar studies using conventional cytogenetics have also indicated the frequent occurrence of spontaneous chromosome fragmentation in cells lacking DNA-PKcs (27, 33). After ionizing radiation, a high number of exchange type aberrations were scored despite the end joining defect, representing 54% of the total break-induced aberrations in DNA-PKcs$^{-/-}$ MEFs (0.772 and 0.018 rejoined aberrations per cell in irradiated DNA-PKcs–deficient and wild-type MEFs, respectively;

Table 1. Spontaneous and radiation-induced chromosome aberrations in DNA-PKcs$^{-/-}$ and wild-type MEFs

DNA-PKcs genotype and dose	No. cells analyzed	Total no. aberrations (frequency/cell)	Break-produced aberrations		No. telomere-telomere fusions (frequency/cell)	No. telomere-DSB fusions (frequency/cell)
			No. nonexchange type aberrations (frequency/cell)	No. exchange type aberrations (frequency/cell)		
+/+, 0 Gy	121	9 (0.074)	8 (0.066)	1 (0.008)	—	—
−/−, 0 Gy	140	44 (0.314)	29 (0.207)	5 (0.036)	10 (0.071)	—
+/+, 2 Gy	55	12 (0.218)	11 (0.200)	1 (0.018)	—	—
−/−, 2 Gy	92	135 (1.467)	59 (0.641)	71 (0.772)	4 (0.043)	1 (0.011)

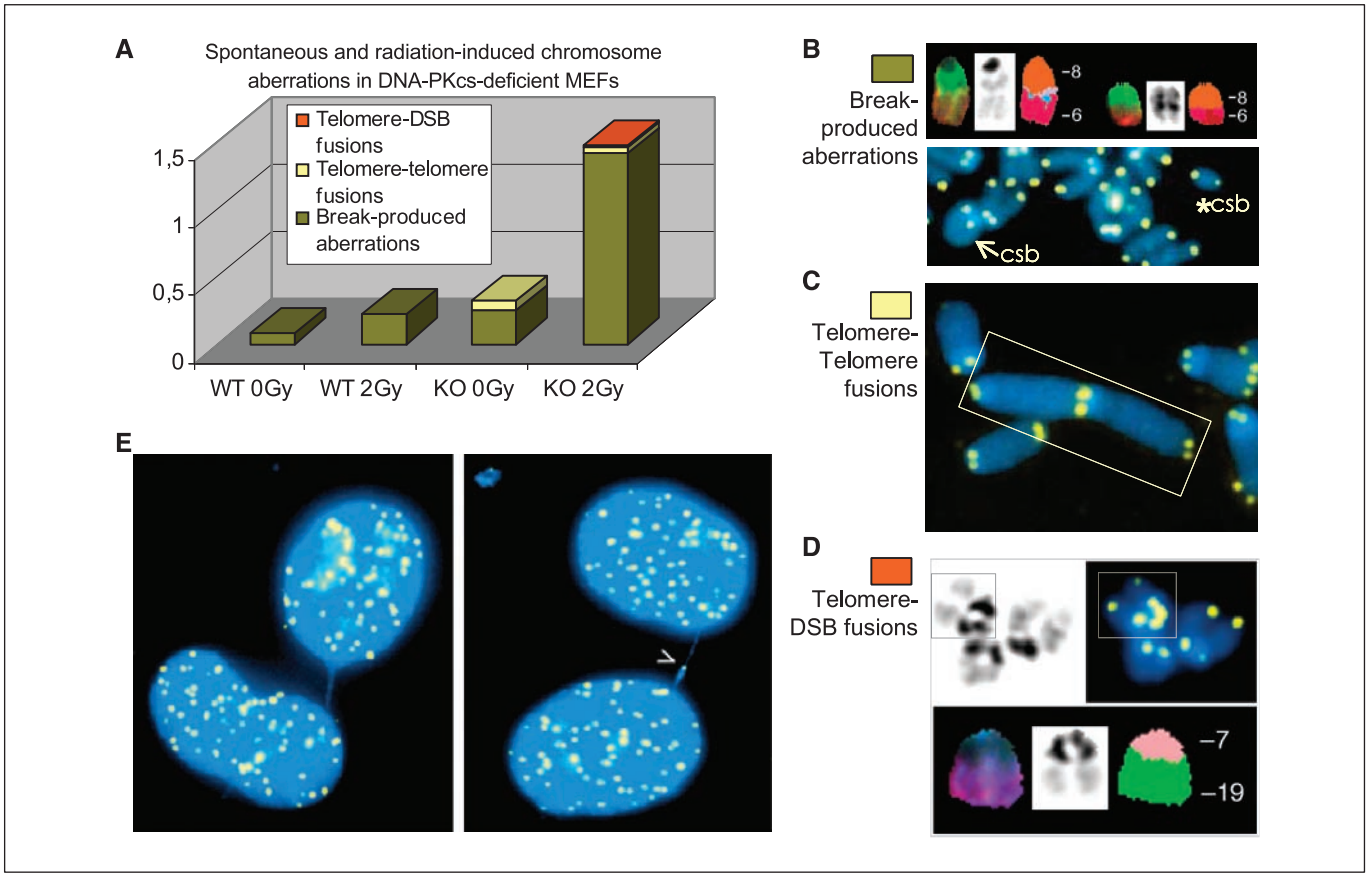

Figure 1. Chromosome aberration formation in DNA-PKcs$^{-/-}$ and DNA-PKcs$^{+/+}$ MEFs. *A,* frequencies of spontaneous and ionizing radiation–induced chromosome aberrations in DNA-PKcs$^{-/-}$ and wild-type MEFs exposed to 0 and 2 Gy of ionizing radiation *in utero* and analyzed *in vitro* as described in Materials and Methods. Chromosome aberrations were classified into break-produced aberrations (*green*), telomere-telomere fusions (*yellow*), or telomere-DSB fusions (*orange*). *B* to *D,* representative examples. Note the high incidence of break-produced aberrations in both nonirradiated and irradiated DNA-PKcs$^{-/-}$ MEFs. On the other hand, under the conditions employed, telomere-DSB fusions are not present in nonirradiated and are rare in irradiated DNA-PKcs$^{-/-}$ MEFs. *B,* examples of break-produced aberrations. *Top row,* exchange-type aberration, specifically a reciprocal translocation between chromosomes 8 and 6 analyzed with SKY-FISH. For each figure, SKY-FISH provides the stained image (*left*), the DAPI reverse image (*middle*), and the pseudocolor image (*right*). *Bottom row,* nonexchange type aberration. *Arrow,* broken centric fragment with only one telomere pair; the resulting acentric fragment with the remaining telomere pair is also present (*asterisk*). *C,* example of a telomere-telomere fusion affecting both chromatids with telomeres present at the fusion point (*white square*). Note the increased strength of the telomeric signals at the fusion point, indicating that in this case the fusion was not associated with erosion in telomere length. *D,* telomere-DSB fusion. *Top row, left,* an inverted DAPI image where an apparently normal chromosome 19 is shown (*black box*). *Right,* when analyzing the telomeric FISH image, three telomeric pairs can be seen. *Bottom row,* SKY-FISH analysis where the chromosomes involved in the rearrangement can be identified: an unbroken chromosome 19, with a complete set of two telomere pairs, has joined to a centric fragment of chromosome 7, which also presents a telomere pair. The telomere pair at the p-arm of chromosome 19 is presumably dysfunctional because it has joined to the broken end of chromosome 7. *E,* examples of nucleoplasmic bridges in binucleated MEFs from irradiated DNA-PKcs$^{+/+}$ (*left*) and DNA-PKcs$^{-/-}$ (*right*) embryos. Irradiated DNA-PKcs$^{+/+}$ derived binucleated MEFs showed a significantly lower frequency of nucleoplasmic bridges than irradiated DNA-PKcs$^{-/-}$ binucleates. Moreover, 3% of binucleates from irradiated DNA-PKcs$^{-/-}$ embryos presented a telomere signal in the bridge (*arrowhead*), presumably resulting from telomere-telomere fusions.

Table 1). Increased formation of exchange-type aberrations has also recently been reported in a DNA-PKcs–deficient human glioblastoma cell line (M059J) after exposure to ionizing radiation (34). In summary, the above results suggest that increased spontaneous chromosome aberrations and radiation sensitivity of primary DNA-PKcs$^{-/-}$ MEFs irradiated *in utero* are mainly due to their DSB repair defect. Telomere dysfunction apparently contributes only marginally to their phenotype.

Sister chromatid joining as an important source of genomic instability in DNA-PKcs$^{-/-}$ mouse embryo fibroblasts. It has been suggested that dicentric chromosomes generated either by DNA breakage or telomeric dysfunction trigger fusion-bridge-breakage cycles through the formation of anaphase bridges. Both telomere-telomere fusions and anaphase bridges occur in tumors and are thought to be important for their clonal evolution and progression (3). To investigate the effect of DNA-PKcs deficiency on genomic instability, we analyzed the formation of nucleoplasmic bridges in binucleated cells using the techniques described under Materials and Methods. Nucleoplasmic bridges are a continuous nucleoplasmic link between the nuclei in a binucleated cell (Fig. 1*E*) and were scored according to the criteria established by Fenech et al. (35). In accordance with a role of DNA-PKcs in genomic stability, we found that DNA-PKcs$^{-/-}$ MEFs show a significantly higher frequency of nucleoplasmic bridges than their wild-type counterparts (0.009 and 0.103 nucleoplasmic bridges per binucleated cell scored for wild-type and DNA-PKcs$^{-/-}$ MEFs, respectively; 539 and 822 binucleated MEFs were scored for wild-type and DNA-PKcs$^{-/-}$ MEFs, respectively; $P \leq 0.001$, χ^2 test).

To examine how impaired DSB repair could affect genomic stability in DNA-PKcs$^{-/-}$ MEFs, we used SKY followed by

centromeric and telomeric labeling to ascertain which chromosome aberrations are potential sources of genomic instability. For this analysis, we first distinguished between two categories of chromosomal rearrangements: conventional rearrangements formed by prereplicative rejoining of two DSBs (translocations, dicentric chromosomes, rings, and interstitial deletions) and rearrangements derived from postreplicative joining of DSBs (isoacentric fragments and isodicentric chromosomes). Table 2 shows the frequencies of these two types of chromosome rearrangements. After irradiation, conventional prereplicative chromosome rearrangements are more frequent in DNA-PKcs$^{-/-}$ than in wild-type MEFs (0.630 and 0.018 per metaphase cell analyzed, respectively). Among the conventional rearrangements observed, dicentric chromosomes contribute to genomic instability when a twist occurs between the two centromeres during division, leading to an anaphase bridge. Strikingly, rearranged chromosomes formed by postreplicative rejoining are only observed in DNA-PKcs$^{-/-}$ MEFs (0.014 and 0.141 per metaphase plate in nonirradiated and irradiated DNA-PKcs$^{-/-}$ MEFs, respectively). Several examples of such aberrations are shown in Fig. 2*A*. In terms of generating genomic instability, isodicentric chromosomes behave like conventional dicentrics.

Isoacentric fragments and isodicentric chromosomes probably derive from breaks that replicated before rejoining, producing thus sister chromatids with breakage at the same location. End joining to each other of these replicated chromatids (sister chromatid fusion) generates isoacentric fragments and isodicentric chromosomes in the subsequent cell division. In most metaphase plates, SKY allowed us to identify the isodicentric chromosome together with a normal homologue. This shows that the isodicentric chromosome did not originate by fusion of homologues but rather by sister chromatid fusion followed by DNA replication. Thus, two divisions after ionizing radiation are required to observe the rearrangements shown in Fig. 2*A*. The 6 hours between ionizing radiation and sacrifice, in addition to the 48 hours allowed for *in vitro* culture, are sufficient to obtain both first and second mitosis. Figure 2*B* shows a scheme of the possible generation of such rearrangements. According to this model, broken chromosomes with fusion of sister chromatids correspond to an intermediate step in the formation of isoacentric and isodicentric rearrangements. Thus, the identification of sister chromatid fusion events would represent an important support for our model. To experimentally test this possibility, we checked whether broken chromosomes with apparent fusion of sister chromatids could be identified in solid-stained first-division metaphases after exposure to 2 Gy. Suspected sister chromatid fusion events were then confirmed by the absence of telomeric signals after telomeric peptide nucleic acid-FISH. A total of 107 broken chromosome ends showed apparent fusion of broken chromatids in the 112 DNA-PKcs$^{-/-}$ MEFs analyzed for this purpose. All sister fusions were confirmed by the absence of telomeric signal at that end (Fig. 2*C*). Sister chromatid fusion affected ~1/3 of the broken ends identified in the DNA-PKcs–deficient background. In contrast, no sister chromatid fusion events were identified in the 128 metaphases analyzed in wild-type MEFs. Altogether, these results provide for the first time evidence that postreplicative joining of DNA DSBs is an important source of chromosome rearrangements contributing to the instability of DNA-PKcs–deficient genomes. Fusion of sister chromatids may result in gene amplification, as first shown by Toledo et al. (36) and Ma et al. (37). In this context, our results—high frequency of sister chromatid fusion and isodicentric chromosome formation in DNA-PKcs–deficient animals—are in accordance with the reported increase in gene amplification in immortal DNA-PKcs$^{-/-}$ rodent cells (38).

Slow rejoining of ionizing radiation–induced double-strand breaks as a potential cause for the increased sister chromatid fusion and other chromosome rearrangement in DNA-PKcs$^{-/-}$ cells. The model of formation of isoacentric and isodicentric aberrations through postreplicative sister chromatid fusion is compatible with a defect in G_1 checkpoint in DNA-PKcs$^{-/-}$ cells that allows chromosomes with unrepaired DSBs to enter S phase and replicate the damage. To investigate this possibility, we measured cell cycle distribution after ionizing radiation in DNA-PKcs$^{-/-}$ MEFs. Similar to wild-type cells, DNA-PKcs$^{-/-}$ cells display a strong arrest in G_1, which is expressed as a strong reduction in the fraction of cells in S phase 8 hours after ionizing radiation (Fig. 3*A*). Moreover, irradiated DNA-PKcs$^{-/-}$ MEFs show a larger G_1/S ratio than DNA-PKcs$^{+/+}$ MEFs (Fig. 3*B*) probably because the persistence of unrepaired DSBs generates a stronger G_1 arrest. These observations are not compatible with a defect in G_1 checkpoint response and suggest that the formation of isoacentric and isodicentric aberrations in DNA-PKcs$^{-/-}$ MEFs cannot be explained by a defect in this checkpoint.

Measurement of the DNA DSBs rejoining in the DNA-PKcs–deficient human glioblastoma cell line M059J showed that these cells are able to rejoin the majority of radiation induced DSBs albeit with slow kinetics (37). Slow rejoining of DSB in DNA-PKcs$^{-/-}$ MEFs could also underlie the increased formation of chromosome rearrangements, particularly those derived from sister chromatid joining (fusion). To examine this possibility, we

Table 2. Chromosome aberrations formed by prereplicative and postreplicative joining of DSBs

DNA-PKcs genotype and dose	Total no. exchange-type aberrations	Rearrangements formed by prereplicative rejoining				Rearrangements formed by postreplicative rejoining		
		Translocations	Dicentric	Interstitial deletions	Total (frequency/cell)	Isoacentric	Isodicentric	Total (frequency/cell)
+/+, 0 Gy	1	—	1	—	1 (0.008)	—	—	0
−/−, 0 Gy	5	—	2	1	3 (0.021)	2	—	2 (0.014)
+/+, 2 Gy	1	—	1	—	1 (0.018)	—	—	0
−/−, 2 Gy	71	27	25	6	58 (0.630)	8	5	13 (0.141)

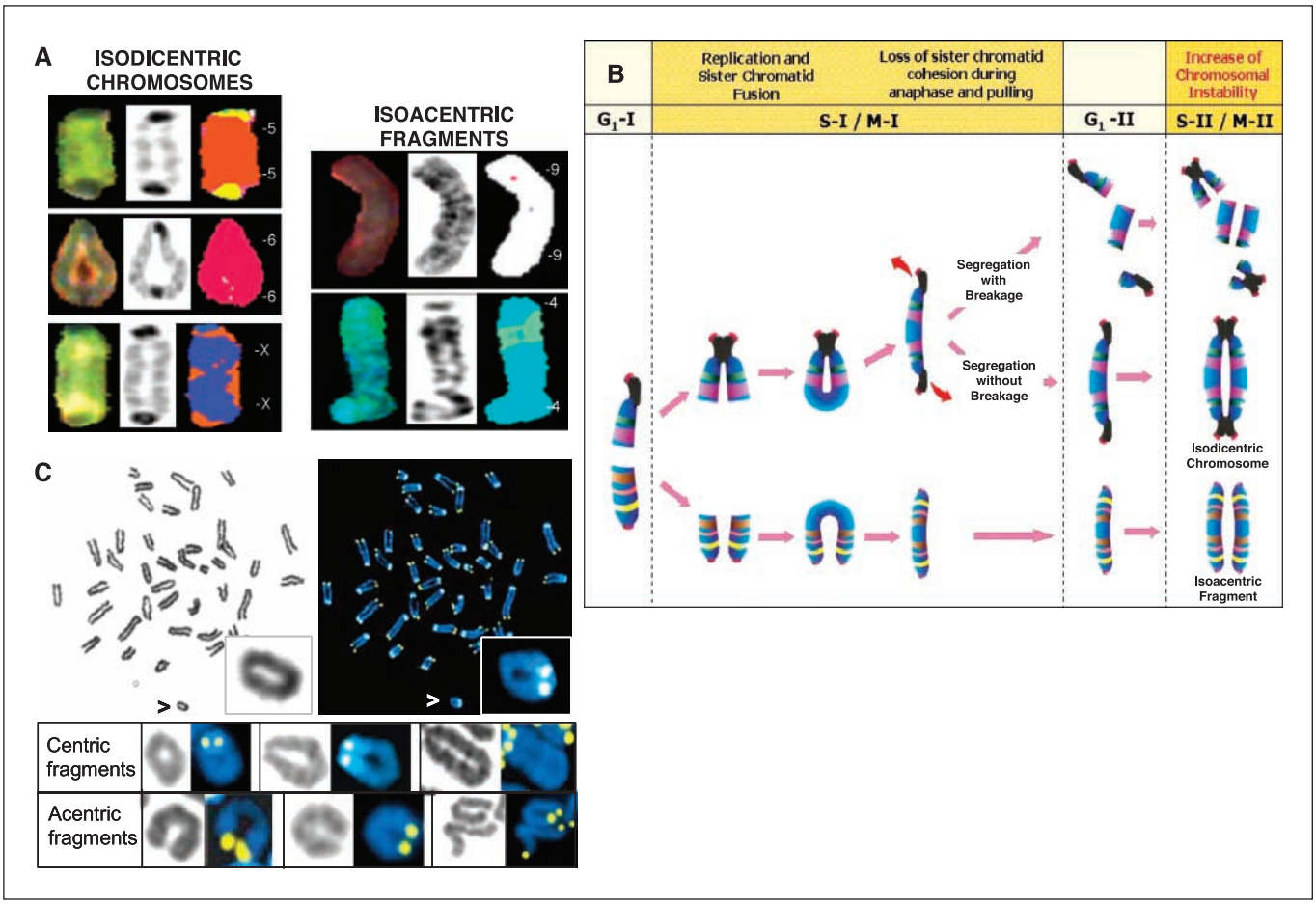

Figure 2. *A,* examples of isodicentric chromosomes (*left*) and isoacentric fragments (*right*) from DNA-PKcs$^{-/-}$ MEFs obtained by SKY-FISH analysis. For cytogenetic analysis, SKY-FISH provides three images: the stained chromosome as seen in the microscope (*left*), the DAPI reverse image (*middle*), and the pseudocolor that the program assigns to each different fluorochrome combination (*right*). *Isodicentric chromosomes, top* to *bottom,* dic(5;5), dic(6;6), and dic(X;X). In most metaphase plates, SKY-FISH allowed us to identify the isodicentric chromosome together with a normal homologue chromosome, thus indicating that isodicentrics did not originate by fusion of homologues but rather by sister chromatid fusion and ulterior DNA replication. *Isoacentric fragments,top,* ace (9;9); *bottom,* ace (4;4). In both isodicentric chromosomes and isoacentric fragments, the DAPI reverse image (*middle*) provides evidence of a duplicated and symmetrical (mirrorlike) banding pattern. *B,* model for the formation of isodicentric chromosomes and isoacentric fragments. A break that occurs in G_1 reaches S phase before rejoining (the chromosome can also be broken in the S phase before replication). After replication, sister chromatids fuse and enter into anaphase. The generated isodicentric chromatids can then enter into fusion-bridge-breakage cycles. Isoacentric chromatids that replicate and progress through the cell cycle, as well as isodicentric chromatids that do not break during anaphase, will generate isoacentric fragments and isodicentric chromosomes, respectively, after the next replication (*S-II/M-II*). Thus, sister chromatid fusion events lead to an increase in chromosome instability by means of gene amplification and accumulation of chromosome aberrations in the following cell divisions. *C, top row,* DNA-PKcs$^{-/-}$ metaphase at first division after irradiation. *Left,* the metaphase has been solid stained with Leishman. *Arrowhead,* a centric fragment of which chromatids are fused; this chromosome fragment is presented at a higher magnification (*inset*) showing evident sister chromatid fusion. After solid staining, a telomeric FISH is applied on the same slides (*right*). In this image, fusion of the chromatids is still evident and absence of telomeres in the q-arms is confirmed. *Bottom two rows,* further examples of centric and acentric fragments where sister chromatids have fused. For each fragment, solid staining evidencing sister chromatid fusion followed by telomeric FISH confirming absence of telomeres in the fused ends is presented.

measured the kinetics of DSB rejoining in irradiated DNA-PKcs$^{-/-}$ and wild-type MEFs by asymmetrical FIGE. The results in Fig. 4*A* indicate a similar linear increase in FAR—a measure of DNA DSBs present—with increasing radiation dose in DNA-PKcs$^{-/-}$ and wild-type MEFs. Because induction of DNA DSBs as a function of radiation dose is thought to be linear, the linear relationship between FAR and radiation dose in the range of interest also implies a linear relationship between FAR and DNA DSBs present. This allows evaluation of DNA DSBs rejoining directly from FAR versus time plots, obviating corrections otherwise required when the relationship between FAR and dose deviates significantly from linearity.

Figure 4 shows the kinetics of DNA DSB rejoining in DNA-PKcs$^{+/+}$ and DNA-PKcs$^{-/-}$ MEFs over a period of 48 hours after exposure to 30 Gy of ionizing radiation. Similar to the results with M059J cells, DNA-PKcs$^{-/-}$ MEFs rejoin the majority of DSBs albeit with slow kinetics. Forty-eight hours after irradiation, the amount of residual breaks in DNA-PKcs$^{-/-}$ is similar to that in control MEFs (Fig. 4*B*). However, at shorter repair times (0.5-6 hours after irradiation), the level of rejoining is strikingly different in the two cell types (Fig. 4*C*). For example, 2 hours after ionizing radiation, most DSBs have been rejoined in wild-type MEFs whereas more than 50% remain unrejoined in DNA-PKcs$^{-/-}$ MEFs (Fig. 4*C*). These results and those reported earlier (39) suggest that DNA-PK deficiency does not prevent joining of DSBs but significantly slows down the kinetics of this rejoining. This alteration in the kinetics could explain our cytogenetic observations as many more DSBs will be present simultaneously for rather long periods of time after

irradiation, increasing thus the probability of interaction between wrong ends, particularly when in close spatial proximity as is the case for sister chromatids.

Discussion

Proteins involved in nonhomologous end joining play an essential role in maintaining genomic stability and in preventing tumor formation (14, 15, 33, 40). Among these proteins, DNA-PKcs serves a dual function: it participates in the repair of DSBs by nonhomologous end joining (for a review, ref. 41) and it contributes to the organization of a functional telomere, thus preventing end joining of whole chromosomes (24, 27, 28). To evaluate the contribution of each of these important functions in protecting the integrity of the genome, we carried out an exhaustive cytogenetic analysis of the spontaneous and ionizing radiation–induced chromosome aberrations in the DNA-PKcs knockout mouse model. We observed a low frequency of telomere-telomere fusions indicative of a limited end-capping defect in our primary DNA-PKcs$^{-/-}$ MEFs. Actually, only one instance of a dysfunctional telomere joined to radiation-induced DSB was found in the entire analysis. We therefore conclude that telomere dysfunction contributes only marginally to radiation sensitivity and genomic instability associated with DNA-PKcs deficiency in primary MEFs. These observations differ from those of Gilley et al. (24) in primary DNA-PKcs$^{-/-}$ MEFs in which higher levels of telomere-telomere fusions ($\sim$20 fusions per 100 cells) were observed than in our study (6 telomere-telomere fusions per 100 cells). The reason for this difference is not clear but may be due to the different population doublings analyzed. In our study, embryos are irradiated *in utero* and the MEFs are analyzed in the first or second population doubling after female sacrifice. In the study by Gilley et al. (24), the MEFs were harvested for analysis after 10 population doublings. It may be important to differentiate between phenotypes of cells maintained in culture over several population doublings and freshly derived MEFs. Further experimentation is required to clarify this issue. Our observations also differ from those of Bailey et al. (30) who showed that transformed *scid* fibroblasts have a strong telomeric phenotype with high rates of telomere-telomere and telomere-DSB fusions. It is likely that this difference in response derives from the transformed phenotype of the cells employed in the latter study and could reflect differences in telomere metabolism or telomere structure between primary and immortalized MEFs as recently suggested by Rebuzzini et al. (42).

Chromosomal rearrangements (exchange-type aberrations) are observed with a high frequency in our DNA-PKcs knockout mouse model and show that despite the repair defect, cells retain substantial DNA end-joining capacity. Similar results have been reported in human cells deficient in DNA-PKcs (34) and in other nonhomologous end joining repair mutants (40). The results of our DSB-rejoining experiments provide an explanation for our cytogenetic observations. Repair-competent cells of higher eukaryotes process DSBs in their genome within minutes using the DNA-PK–dependent nonhomologous end joining apparatus. However, cells with defects in this repair pathway, such as M059J (39) and DNA-PKcs$^{-/-}$ MEFs (Fig. 4), use a backup pathway operating with slow kinetics to remove the majority of DSBs. In the slowly repairing DNA-PKcs$^{-/-}$ MEFs, many DSBs will remain as repair substrates relatively close in space and time. As a consequence, the probability of misjoining will increase, leading to the formation of chromosome rearrangements. The longer the DSBs remain unrepaired, the higher the probability of interaction and formation of chromosome aberrations, suggesting that chromosome territories in the interphase nucleus are dynamic and capable of interaction. The nature of the pathway responsible for DNA DSB

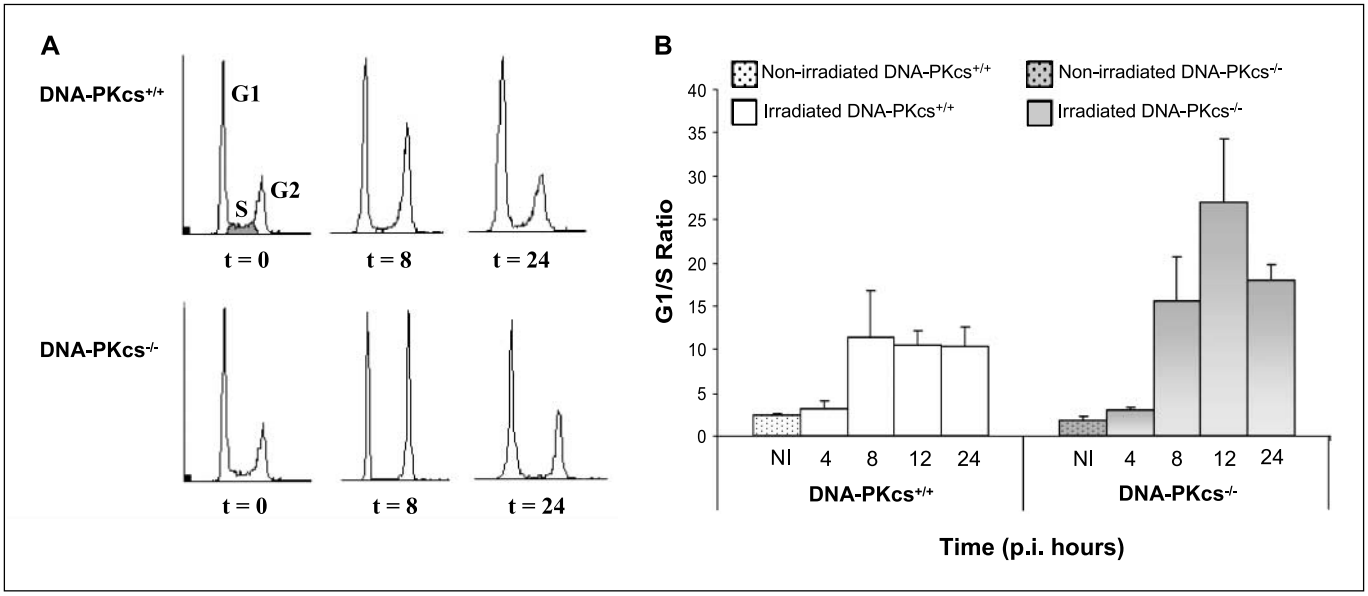

Figure 3. Activation of the G_1 checkpoint in DNA-PKcs$^{-/-}$ MEFs. Primary DNA-PKcs$^{+/+}$ and DNA-PKcs$^{-/-}$ MEFs were prepared from 12- to 14-day-old embryos and grown in culture for two to four doublings. Exponentially growing cultures were exposed to 7-Gy ionizing radiation or left unirradiated and returned to 37°C. At various times thereafter, cells were collected and analyzed by flow cytometry. *A,* flow cytometry profiles obtained at 0, 8, and 24 hours after irradiation. Note the depletion of S-phase cells at 8 hours and to a lesser extent at 24 hours after irradiation, which is a manifestation of the activation of the G_1 checkpoint, both in DNA-PKcs$^{+/+}$ and DNA-PKcs$^{-/-}$ MEFs. *B,* the ratio of the fraction of cells in G_1 and S (G_1/*S Ratio*) at different times after irradiation is presented. Arrest in G_1 manifests as an increase in this ratio and is evident for both cell types starting at 8 hours and reaching a peak at 8 to 12 hours after irradiation. *Columns,* mean from three different experiments; *bars,* SE.

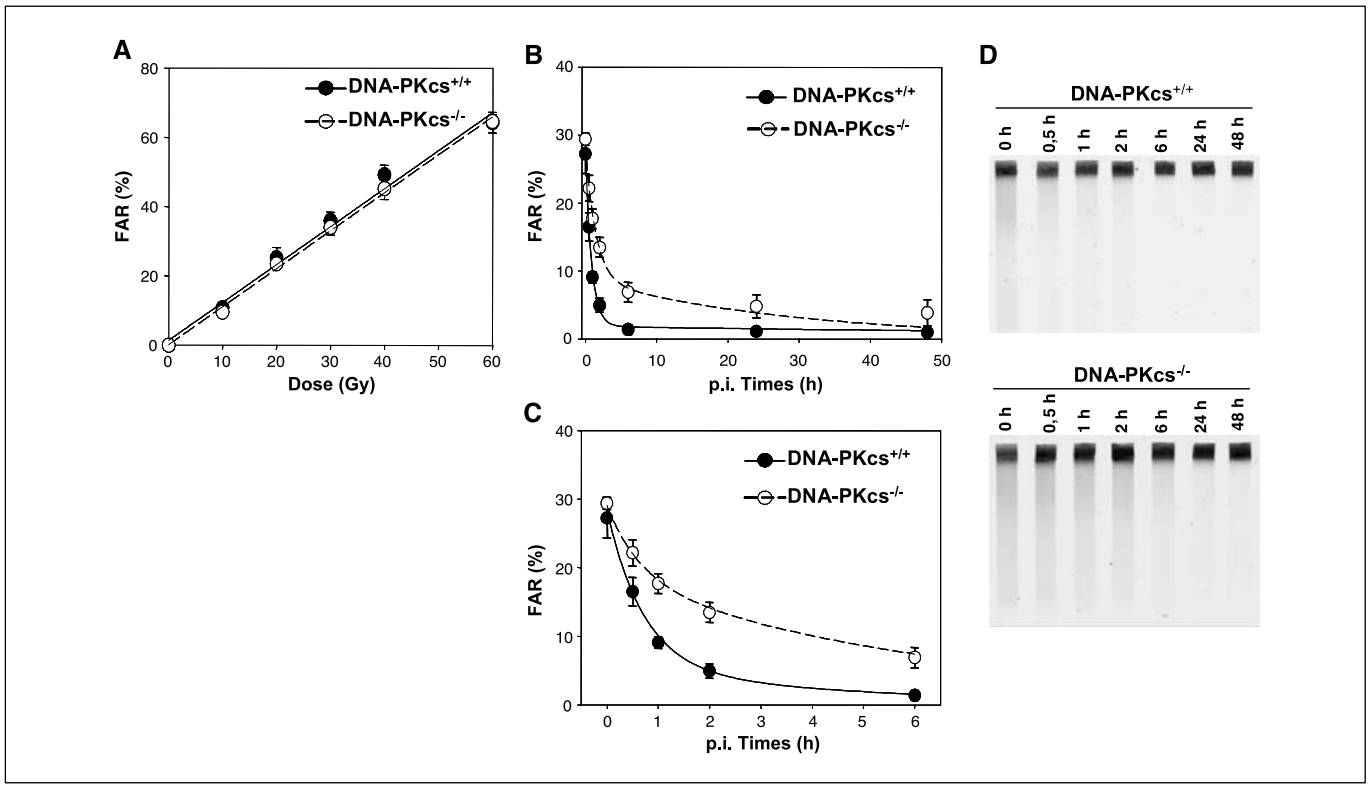

Figure 4. *A,* FAR as a function of radiation dose in the range of 0 to 60 Gy for DNA-PKcs$^{+/+}$ and DNA-PKcs$^{-/-}$ MEFs. MEFs were prepared from 12- to 14-day-old embryos and used for experiments after two to four cell doublings, subsequent to reaching confluence. Both types of MEFs showed an equal and approximately linear increase in FAR with increasing dose of radiation. *Points,* mean of two determinations from three independent experiments; *bars,* SD. *B,* repair kinetics for irradiated MEFs allowed to repair for up to 48 hours. Note the slower kinetics of end joining in DNA-PKcs$^{-/-}$ MEFs but also that after 24 hours, the majority of the DSBs had been rejoined. *C,* repair kinetics during the first 6 hours after irradiation. *Points,* mean of two determinations from three independent experiments; *bars,* SD. *D,* typical asymmetrical FIGE gels of the kinetics of DSB rejoining in DNA-PK$^{-/-}$ and DNA-PKcs$^{+/+}$ MEFs.

rejoining in the absence of DNA-PKcs has not been elucidated completely (43). Although homologous recombination is an obvious candidate and has been actually shown to be stimulated in nonhomologous end joining–defective cells (44), an extensive study using DT40 cells did not support this possibility (45). In these cells, rejoining of ionizing radiation–induced DNA DSBs follows a kinetics similar to those of other cells of higher eukaryotes despite the 1,000-fold increase in their ability to carry out homologous recombination. In addition, DSB rejoining remained unchanged in knockout mutants with defects in Rad51, Rad51B, Rad52, or Rad54, and a Rad54 defect in a Ku70-deficient mutant remained without effect on DSB rejoining. It is therefore possible that an inherently slow nonhomologous end joining repair pathway operating independently of DNA-PK and DNA ligase IV/XRCC4 underlies the observed DSB rejoining in DNA-PK MEFs. Recent studies implicate DNA ligase III and poly(ADP-ribose) polymerase 1 in this pathway of end joining (43, 46). In favor of a DNA-PK–independent alternative pathway of nonhomologous end joining, our results show that its function is associated with the joining of incorrect ends, an effect not compatible with homologous recombination.

The most striking and novel observation here is that chromosome aberrations formed by postreplicative rejoining are likely to make an important contribution to the radiosensitivity and chromosome instability of DNA-PKcs$^{-/-}$ MEFs. Chromosome aberrations resulting from postreplicative joining were only observed in DNA-PKcs$^{-/-}$ MEFs although the initial numbers of breaks produced after irradiation were similar in the two genetic backgrounds as shown by the asymmetrical FIGE experiments (Fig. 4*A*). Sister chromatid fusion can result from a variety of dysfunctions. In telomerase-deficient cells and mice, replication-dependent telomere erosion during S phase causes unprotection of both chromatids at the same time, leading frequently to postreplicative end joining of sister chromatids (22). Moreover, the status of cell cycle checkpoints could also influence the occurrence of sister chromatid fusion as checkpoints will block the progression through the cell cycle of cells containing broken chromosomes. In a G_1 checkpoint–deficient genetic background, cells with DSBs progress into S phase, generating a broken sister chromatid that favors sister chromatid fusion. Indeed, sister chromatid fusion leading to isodicentric chromosomes and inverted repeats is a characteristic of mouse embryonic stem cells (47) and of the ES-30 cancer cell line (48), both of which lack the G_1 p53-dependent cell cycle checkpoint (47–50). In the case of DNA-PKcs–deficient MEFs, which possesses wild-type ATM and p53, our flow cytometry experiments failed to detect defects in the G_1 checkpoint response. Other studies with the DNA-PKcs$^{-/-}$ mouse model also confirm the G_1 checkpoint response after DNA damage, manifested by a depletion of S-phase cells and an increase in the G_1/S ratio after ionizing radiation (51, 52). To explain the formation of isoacentric fragments and isodicentric chromosomes by sister chromatid fusion in DNA-PKcs$^{-/-}$ MEFs, it should be taken into consideration that irradiation was done *in vivo* on an unsynchronized cell population. Thus, a fraction of cells in the mouse embryos was irradiated in S phase. Mounting evidence points

to a role for DNA-PKcs in damage-induced S-phase arrest and its reversal (53–56). Damage-induced S-phase arrest was reversed *in vitro* by the addition of a DNA-PK inhibitor or by immunodepletion of DNA-PKcs, suggesting that DNA-PKcs may be directly involved in S-phase checkpoint through modulation of replication proteins (53, 55). In this scenario, isoacentric and isodicentric rearrangements can be originated from individual DNA DSBs that progress through S phase, due to compromised damage-induced S-phase checkpoint, and generate two sister chromatids with breakage at the same site. Throughout G_2, sister chromatid cohesion may prevent free break ends from long-term diffusion (57). Favored by proximity, these broken sister chromatids can fuse and progress through the cell cycle until the next S phase and subsequent mitosis, when isoacentric and isodicentric rearrangements are observed.

In conclusion, our results show that in the absence of DNA-PKcs, broken DNA ends are processed with slow kinetics and the long-lived ends interact with other DNA ends in the vicinity before or after replication, causing the formation of exchange-type chromosome aberrations. Thus, the ability of cells to quickly and efficiently remove DSBs may, together with a correct S-phase checkpoint, play a major role in maintaining the stability of the genome in unirradiated cells and in preventing the formation of lethal chromosome aberrations in cells exposed to agents inducing this type of lesion.

Acknowledgments

Received 3/21/2005; revised 8/2/2005; accepted 9/14/2005.

Grant support: European Union grant FI-CT-2003-508842; Comisión Interministerial de Ciencia y Tecnología grants 2001-SGR-00202 and SAF2002-11833-E (L. Tusell and A. Genescà); Ministerio de Ciencia y Tecnología grants SAF2001-1869 and GEN2001-4856-C13-08, Regional Government of Madrid grant 08.1/0054/01, European Union grants INTACT LSHC-CT-2003-506803, ZINCAGE FOOD-CT-2003-506850, and RISC-RAD FI6R-CT-2003-508842, and Josef Steiner Award 2003 (M.A. Blasco); Deutsche Forschungsgemeinschaft, Germany (G. Iliakis); European Union grant TELOSENS FIGH-CT-2002-00217 (G. Iliakis, A. Genescà, and M.A. Blasco); and Human Frontier Science Program Organization (G. Taccioli).

The costs of publication of this article were defrayed in part by the payment of page charges. This article must therefore be hereby marked *advertisement* in accordance with 18 U.S.C. Section 1734 solely to indicate this fact.

We thank R. Serrano and E. Santos for mouse care and genotyping, I. Ponsa for advice in the evaluation of binucleated cells, R. Eguia for advice with SKY analysis, F. Windhofer for advice with asymmetrical FIGE, N. Agell for advice with flow cytometry, M. Puigcerver for technical assistance, and *SiMTRAD* at the Universitat Autònoma de Barcelona School of Modern Languajes for editing of the manuscript.

References

1. Lengauer C, Kinzler KW, Vogelstein B. Genetic instabilities in human cancers. Nature 1998;396:643–9.
2. Lengauer C, Kinzler K, Vogelstein B. Genetic instability in colorectal cancers. Nature 1997;386:623–7.
3. Gisselsson D, Pettersson L, Houglund M, et al. Chromosome breakage-fusion-bridge events cause genetic intratumor heterogeneity. Proc Natl Acad Sci U S A 2000;97:5357–62.
4. Ribas M, Masramon L, Aiza G, Capellà G, Miró R, Peinado MA. The structural nature of chromosomal instability in colon cancer cells. FASEB J 2003;17:289–91.
5. Aaltonen LA, Peltomaki P, Leach FS, et al. Clues to the pathogenesis of familial colorectal cancer. Science 1993; 260:812–6.
6. Ionov Y, Peinado MA, Malkhosyan S, Shibata D, Perucho M. Ubiquitous somatic mutations in simple repeated sequences reveal a new mechanism for colonic carcinogenesis. Nature 1993;363:558–61.
7. Thibodeau SN, Bren G, Schaid D. Microsatellite instability in cancer of the proximal colon. Science 1993; 260:816–9.
8. Liu B, Parsons R, Papadopoulos N, et al. Mismatch gene repair defects in sporadic colorectal cancers with microsatellite instability. Nat Genet 1996;2:169–74.
9. Kraemer KH, Lee MM, Scotto J. DNA repair protects against cutaneous and internal neoplasia: evidence from xerodermal pigmetosum. Carcnogenesis 1984;5:511–4.
10. Jackson SP. Sensing and repairing DNA double-strand breaks. Carcinogenesis 2002;23:687–96.
11. Doherty AJ, Jackson SP. DNA repair: how KU makes ends meet. Curr Biol 2001;11:R920–024.
12. Thompson LH, Shild D. Homologous recombinational repair of DNA ensures mammalian chromosome stability. Mutat Res 2001;477:131–53.
13. Li GC, Ouyang HH, Li XL, et al. Ku70: a candidate tumor suppressor gene for murine T cell lymphoma. Mol Cell 1998;2:1–8.
14. Difilippantonio MJ, Zhu J, Chen HT, et al. DNA repair protein Ku 80 suppresses chromosomal aberrations and malignant transformation. Nature 2000;404:510–4.
15. Gao Y, Ferguson DO, Xie W, et al. Interplay of p53 and DNA-repair protein XRCC4 in tumorigenesis, genomic stability, and development. Nature 2000;404:897–900.
16. Riballo E, Critchlow SE, Teo SH, et al. Identification of a defect in DNA ligase IV in a radiosensitive leukaemia patient. Curr Biol 1999;9:699–702.
17. O'Driscoll M, Gennery AR, Seidel J, Concannon P, Jeggo PA. An overview of three new disorders associated with genetic instability: LIG4 syndrome, RS-SCID and ATR-Seckel syndrome. DNA Repair (Amst) 2004;3:1227–35.
18. Moshous D, Callebaut I, de Chasseval R, et al. Artemis, a novel DNA double-strand break repair/V(D)J recombination protein, is mutated in human severe combined immune deficiency. Cell 2001;105:177–86.
19. Kobayashi N, Agematsu K, Sugita K, et al. Novel artemis gene mutations of radiosensitive severe combined immunodeficiency in Japanese families. Hum Genet 2003;112:348–52.
20. Moshous D, Pannetier R, Chasseval RD, et al. Partial T and B lymphocyte immunodeficiency and predisposition to lymphoma in patients with hypomorphic mutations in Artemis. J Clin Invest 2003;111:381–7.
21. O'Driscoll M, Cerosaletti KM, Girard P-M, et al. DNA ligase IV mutations identified in patients exhibiting development delay and immunodeficiency. Mol Cell 2001;8:1175–85.
22. Blasco MA, Lee HW, Hande MP, et al. Telomere shortening and tumor formation by mouse cells lacking telomerase RNA. Cell 1997;91:25–34.
23. Artandi SE, Chang S, Lee S-L, et al. Telomere dysfunction promotes non-reciprocal translocations and epithelial cancers in mice. Nature 2000;406:641–5.
24. Gilley D, Tanaka H, Hande MP, et al. DNA-PKcs is critical for telomere capping. Proc Natl Acad Sci U S A 2001;98:15084–8.
25. d'Adda di Fagagna F, Reaper PM, Clay-Farrace L, et al. A DNA damage checkpoint response in telomere-initiated senescence. Nature 2003;426:194–8.
26. Takai H, Smogorzewska A, de Lange T. DNA damage foci at dysfunctional telomeres. Curr Biol 2003; 13:1549–56.
27. Bailey SM, Meyne J, Chen DJ, et al. DNA double-strand break repair proteins are required to cap the ends of mammalian chromosomes. Proc Natl Acad Sci U S A 1999;96:14899–904.
28. Goytisolo FA, Samper E, Edmonson S, Taccioli GE, Blasco MA. The absence of the DNA-dependent protein kinase catalytic subunit in mice results in anaphase bridges and in increased telomeric fusions with normal telomere length and G-strand overhang. Mol Cell Biol 2001;21:3642–51.
29. Latre L, Tusell L, Martín M, et al. Shortened telomeres join to DNA breaks interfering with their correct repair. Exp Cell Res 2003;287:282–8.
30. Bailey SM, Cornforth MN, Ullrich RL, Goodwin EH. Dysfunctional mammalian telomeres join with DNA double-strand breaks. DNA Repair (Amst) 2004;3:349–57.
31. Taccioli GE, Amatucci AG, Beamish HJ, et al. Targeted disruption of the catalytic subunit of the DNA-PK gene in mice confers severe combined immunodeficiency and radiosensitivity. Immunity 1998;9:355–66.
32. Martin M, Genescà A, Latre L, et al. Radiation-induced chromosome breaks in AT cells remain open. Int J Radiat Biol 2003;79:203–10.
33. Karanjawala ZE, Grawunder U, Hsieh CL, Lieber MR. The nonhomologous DNA end joining is important for chromosome stability in primary fibroblasts. Curr Biol 1999;9:1501–4.
34. Virsik-Köpp P, Rave-Fränk M, Hofman-Hüther H, Schmidberger H. Role of DNA-PK in the process of aberration formation as studied in irradiated human glioblastoma cell lines M059K and M059J. Int J Radiat Biol 2003;79:61–8.
35. Fenech M, Chang WP, Kirsch-Volders M, Holland M, Bonassi S, Zeiger E. HUMN project: detailed description of the scoring criteria for the cytokinesis-block micronucleus assay using isolated lymphocyte cultures. Mut Res 2003;534:65–75.
36. Toledo F, Le Roscouet D, Buttin G, Debatisse M. Coamplified markers alternate in megabase long chromosomal inverted repeats and cluster independently in interphase nuclei at early steps of mammalian gene amplification. EMBO J 1992;11:2665–73.
37. Ma C, Martin S, Trask B, Hamlin JL. Sister chromatid fusion initiates amplification of the dihydrofolate reductase gene in Chinese hamster cells. Genes Dev 1993; 7:605–20.
38. Mondello C, Rebussini P, Dolzan M, Edmondson S, Taccioli GE, Giulotto E. Increased gene amplification in immortal rodent cells deficient for the DNA-dependent protein kinase catalytic subunit. Cancer Res 2001;61: 4520–5.
39. DiBiase SJ, Zeng Z-C, Chen R, Hyslop T, Curran WJ, Iliakis G. DNA-dependent protein kinase stimulates an independently active, nonhomologous, end-joining apparatus. Cancer Res 2000;60:1245–53.
40. Ferguson DO, Sekiguchi JM, Chang S, et al. The nonhomologous end-joining pathway of DNA repair is required for genomic stability and the suppression of translocations. Proc Natl Acad Sci U S A 2000;97:6630–3.
41. Smith GCM, Jackson SP. The DNA-dependent protein kinase. Genes Dev 1999;13:916–34.
42. Rebuzzini P, Lisa A, Giulotto E, Mondello C. Chromosomal end-to-end fusions in immortalized mouse embryonic fibroblasts deficient in the DNA-dependent protein kinase catalytic subunit. Cancer Lett 2004;203:79–86.

43. Wang H, Rosidi B, Perrault R, et al. DNA ligase III as a candidate component of back up pathways of nonhomologous end joining. Cancer Res 2005;65:4020–30.

44. Delacote F, Han M, Stamato TD, Jasin M, Lopez BS. An xrcc4 defect or Wortmannin stimulates homologous recombination specifically induced by double-strand breaks in mammalian cells. Nucleic Acids Res 2002;30: 3454–63.

45. Wang H, Zeng ZC, Bui TA, et al. Efficient rejoining of radiation-induced DNA double-strand breaks in vertebrate cells deficient in genes of the RAD52 epistasis group. Oncogene 2001;20:2212–24.

46. Audebert M, Salles B, Calsou P. Involvement of poly(ADP-ribose) polymerase-1 and XRCC1/DNA ligase III in an alternative route for DNA double-strand breaks rejoining. J Biol Chem 2004;279:55117–26.

47. Lo AW, Sprung CN, Fouladi B, et al. Chromosome instability as a result of double-strand breaks near telomeres in mouse embryonic stem cells. Mol Cell Biol 2002a;22:4836–50.

48. Lo AW, Sabatier L, Fouladi B, Pottier G, Ricoul M, Murnane JP. DNA amplification by breakage/fusion/bridge cycles initiated by spontaneous telomere loss in a human cancer cell line. Neoplasia 2002b;4:531–8.

49. McIlwrath AJ, Vasey PA, Ross GM, Brown R. Cell cycle arrest and radiosensitivity of human tumor cell lines: dependence on wild-type p53 for radiosensitivity. Cancer Res 1994;54:3718–22.

50. Aladjem MI, Spike BT, Rodewald LW, et al. ES cells do not activate p53-dependent stress responses and undergo p53-independent apoptosis in response to DNA damage. Curr Biol 1998;8:145–55.

51. Burma S, Kurimasa A, Xie G, et al. DNA-dependent protein kinase-independent activation of p53 in response to DNA damage. J Biol Chem 1999;274:17139–43.

52. Jimenez GS, Bryntesson F, Torres-Arzayus MI, et al. DNA-dependent protein kinase is not required for the p53-dependent response to DNA damage. Nature 1999; 400:81–3.

53. Park JS, Park SJ, Peng X, Wang M, Yu MA, Le SH. Involvement of DNA-dependent protein kinase in UV-induced replication arrest. J Biol Chem 1999;274: 32520–7.

54. Wang Y, Zhou XY, Wang H, Huq MS, Iliakis G. Roles of replication protein A and DNA-dependent protein kinase in the regulation of DNA replication following DNA damage. J Biol Chem 1999;274:22060–4.

55. Wang H, Guan J, Wang H, Perrault AR, Wang Y, Iliakis G. Replication protein A2 phosphorylation after DNA damge by the coordinated action of ataxia telangiectasia-mutated and DNA-dependent protein kinase. Cancer Res 2001;61:8554–63.

56. Guan J, DiBiase S, Iliakis G. The catalytic subunit DNA-dependent protein kinase (DNA-PKcs) facilitates recovery from radiation-induced inhibition of DNA replication. Nucleic Acids Res 2000;28:1183–92.

57. Sjogren C, Nasmyth K. Sister chromatid cohesion is required for postreplicative double-strand break repair in *Saccharomyces cerevisiae*. Curr Biol 2001;11: 991–5.